Do slow slip earthquakes inhibit catastrophes? Geologic evidence from the Guerrero segment, Mexican subduction zone

María-Teresa Ramírez-Herrera[1*], Jan Cerny[1,2], Nestor Corona[3], Krzysztof Gaidzik[4], Daisuke Sugawara[5], Steven L. Forman[6], M. Luisa Machain-Castillo[7], Avto Gogichaishvili[8]

*Corresponding Author

1. Laboratorio de Tsunamis y Paleosismología, Instituto de Geografía, Universidad Nacional Autónoma de México
2. Laboratorio de Tsunamis y Paleosismología, Instituto de Geografía, Universidad Nacional Autónoma de México. (Current address: Institute of Geology of the Czech Academy of Sciences, Prague, Czech Republic)
3. COLMICH, Centro de Estudios de Geografía Humana, Michoacán, México
4. Institute of Earth Sciences, University of Silesia, Poland
5. Museum of Natural and Environmental History, Shizuoka, Japan (Current address: International Research Institute of Disaster Science, Tohoku University, Japan)
6. Department of Geosciences, Baylor University, USA
7. Instituto de Ciencias del Mar y Limnología, Universidad Nacional Autónoma de México
8. Instituto de Geofísica Unidad Morelia, Universidad Nacional Autónoma de México

This paper is a non-peer reviewed preprint submitted to EarthArXiv. This preprint was submitted to Nature Communications journal for peer review on 4th May 2023.

Twitter: @TeresaRamirezH

Abstract

Globally, the largest tsunamigenic earthquakes have occurred along subduction zones. The Mw>9 devasting events in Chile, Sumatra, and Japan struck in areas where no instrumental records reported similar events. The one-thousand kilometer-long Mexican subduction zone (MSZ), where the Rivera-Cocos plates subduct under the North American plate, has no records of events of such magnitude. Historical and geologic evidence suggests the occurrence of a Mw8.6 tsunamigenic earthquake in the MSZ. However, the Guerrero segment (GS) has not experienced a large event in over 100 years. Several hypotheses have been proposed to explain this, e.g., slow slip events (SSEs) and the rheology of this segment favoring slow slip over rapid slip. However, none of these hypotheses have been confirmed with evidence. Here, we show geologic evidence that reveals a ca. 2000-year history of large tsunamigenic earthquakes and demonstrate that a Mw>8 event occurred ca. AD 1300 in this segment of the MSZ, indicating a long and variable earthquake recurrence (> 700 years). This evidence prompts the assessment of earthquake and tsunami potential using long-term evidence combined with instrumental observations along the MSZ and other subduction zones.

Keywords: earthquakes, tsunami deposits, subduction, Guerrero segment, slow slip

Globally, high-magnitude (> 8 Mw) earthquakes often occur along subduction zones, such as in Chile in 1960, Sumatra in 2004, and Japan in 2010. The Guerrero segment (GS), an approximately 200 km-long part of the Mexican subduction zone (MSZ), is known for low seismic activity and is often referred to as the Guerrero Seismic Gap (Fig. 1a, b). A proposed plausible rupture of the entire gap could generate an earthquake of Mw>8.4[1]. An earthquake scenario of such magnitude would affect the Mexico City metropolitan area with more than 22 million people. A catastrophic tsunami accompanying this earthquake could cause significant damage to coastal communities such as Acapulco, among others. Recent studies suggest that slow slip events (SSEs) may prevent the occurrence of large earthquakes in the GS[2,3]. In turn, the rheology on this segment of the MSZ promotes slow slip over fast slip, with earthquake generation at the plate interface[3]. However, this hypothesis is based on an incomplete assessment of tsunamigenic earthquakes historically and in the late Holocene. Indeed, there are other subduction zones where large earthquakes and SSEs have occurred in the same or neighboring sectors of subduction zones, such as the Japan subduction zone[4,5,6].

Here, we present geologic evidence that reveals a ca. 2000-year history of large tsunamigenic earthquakes and demonstrate that Mw>8 tsunamigenic events occurred in the past in the GS, with a long and variable recurrence (> 700 years). Our data suggest a likelihood for their future occurrence. Furthermore, we discuss possible relations between slow and rapid slip, revealing that SSEs of the MSZ do not yield sufficient strain release to mute large earthquakes or prevent catastrophic earthquakes and tsunamis from occurring in this segment and neighboring segments.

Coastal and offshore morphology

The Guerrero segment of the MSZ, between Acapulco and Petatlán (Figure 1a, b), has been defined as a morphotectonic zone[8] characterized onshore by a series of coastal lagoons, sand bars, beach ridges, alluvial plains, and rocky promontories[7]. The morphology offshore shows a narrow shelf, 7–12 km in width[8], and a trench extending ~70 km from the coastline. Several morphologic features characterize the rough offshore topography, e.g., popped-up mountains, seamounts, ridges, and escarpments, which are associated in other regions with shallow megathrust earthquakes and tsunamis[9,10]. The coast near Acapulco is wave-dominated and microtidal, ranging from 0.6 m to -0.3 m[11].

We focused on a low coastal alluvial plain in search for evidence of historical and prehistorical tsunamis and their triggering earthquakes (Fig. 1c). Previous studies infer late- and mid-Holocene earthquakes and associated tsunamis[7,12]. Here, we describe sites with excavations at a shoreline-normal transect (Fig. 1c; Supplementary material Supplementary Fig. S1) with a focus on the A1 and A2 sites. The A1 site is located on a lowland, covered by grasses, at the edge of an ancient estuary partially fringed by mangroves, and ~2 m above mean sea level (amsl). Seaward, the landscape is represented by a series of beach ridges and swales, swamps, mangrove marshes, sand dunes up to 5 m high, and a steep beach with cups. Site A2 is located along the same transect as site A1 and in a similar geomorphic setting but with a slightly higher up slope.

Geologic evidence of large earthquakes and tsunamis

We discovered robust evidence for past large tsunamigenic earthquakes that provides a needed context to evaluate the potential for future equivalent events in this sector of the MSZ. The local geology and topography indicate that the study site is currently in an estuary at a distance of ~800 m from the shoreline and 2 m above sea level, providing a higher preservation potential of tsunami deposits.

Three sand units are revealed by stratigraphic logs for sites A1 and A2 that may be associated with past tsunami events. Sand unit 1 in log A2 is apparently an artifact produced by landscape denudation from recent human activities and yields a near modern ^{14}C age of 1989–1992 cal AD (Fig. 2; Supplementary Table S1, S2, S3). Radiocarbon ages are inverted with depth and may reflect burrowing and bioturbation[13]. Sand unit 2 is observed at both the A1 and A2 sites (Fig. 2; Supplementary Fig. S2) and contains unique taxa of marine diatoms that are absent in units above and below (Fig. 3). These diatoms are not well preserved and are scarce, and laboratory procedures have been used to enhance diatom detection[14]. Furthermore, the elemental composition of this unit shows an increase in Na, Mg, Ca, Br and Ba, indicating a marine influence (Supplementary Fig. S3). The clay unit below also shows abundant diatoms indicative of a brackish environment, while the clay with sand unit above shows a significant decrease in brackish diatoms, from 60% to 10%, suggesting a land-level change, probably with coastal coseismic uplift (Fig. 3).

The anisotropy of magnetic susceptibility (AMS) was used to characterize the sediment fabric, confirm the occurrence of a high-energy event, and reconstruct the flow characteristics of a suspected tsunami. AMS results show magnetic fabric (MF I) with a significant degree of anisotropy *P* and anomalous orientation of $\mathbf{K_1}$ (not perpendicular to the shoreline) in sand unit 2

(Fig. 4), suggesting deposition in a high-energy environment during a tsunami inundation event. River inundation is excluded by the presence of marine diatoms and geochemical salinity indicators. This interpretation is consistent with a significant increase in magnetic susceptibility at the bottom of unit 2, reflecting swash processes sorting for the heavier magnetic grains, with a linear decrease upward, as depositional energy slackens, as normal grading of the unit (Fig. 4). The different mechanical properties of sediments (particle size and shape) likely explain why $\mathbf{K_1}$ lacks reorientation perpendicular to the MF flow direction, despite exhibiting a higher degree of anisotropy. MF II from the clay unit below is typical of sedimentary MF of a low-energy depositional environment with mixed horizontal $\mathbf{K_1}$ and $\mathbf{K_2}$ components and a low degree of anisotropy P[15]. Radiocarbon ages from sand unit 2 at both A1 and A2 sites yielded similar ages of 1955–1956 cal AD and 1954–1955 cal AD, respectively. Instrumental records report three earthquakes and tsunamis in the late 1950s to early 1960s that may be related to this sand deposit. The M 7.8 earthquake produced a tsunami near Acapulco in 1957, although tide gauge data at the Acapulco port did not confirm a permanent uplift produced by this earthquake[16]. The 11 May 1962 (M 7.1) and 19 May 1962 (M 7.0) tsunamigenic earthquakes (Fig. 1) produced permanent uplift of 15±3 cm and 7±3 cm during these events in the Acapulco region[16]. Sand unit 2 is likely associated with the 1957 earthquake and tsunami.

Sand Unit 3 is observed on both A1 and A2 and shows a sharp basal contact and flame structures indicating syndepositional soft-sediment deformation. This unit also includes broken shells and fragmented and whole marine diatom valves (Fig. 3), suggesting marine inundation by a tsunami. Sediments above sand unit 3 are composed of clayish silt with predominantly brackish diatoms (> 40%), while sediments below are composed of fine sand with less fragmented diatom valves and

few brackish diatoms (< 5%). This sudden change in the environment suggests land subsidence. Based on the analysis of diatoms in the current topography and coastal environments at the site (Figs. 5, S4), the drop in land level could be equivalent to a change from a beach ridge elevation to an estuary or a swale elevation, likely a subsidence in the range of ≥ 1 m. We suggest that a large earthquake, Mw>8, produced the observed coseismic coastal subsidence and triggered a tsunami, flooding at least 800 m inland. A slight reorientation tendency of $\mathbf{K_1}$ to the perpendicular position and a slightly higher degree of anisotropy *P* suggest that sand unit 3 was deposited in a higher-energy environment[17,18,19,20]. The age of this event through OSL dating of quartz grains indicates that this earthquake and tsunami occurred between 1240 and 1370 AD (Supplementary Table S3). The earliest historical documents written in Spanish record earthquakes that occurred in the 15th century[21] and the oldest historical tsunamigenic event recorded on the GS date to 1537 AD[22]. Thus, historical records do not, but our results using different proxies demonstrate that a large tsunamigenic earthquake occurred on the Guerrero coast between 1240 and 1370 AD.

Sand unit 4 is composed mainly of fine sand and shows a sharp basal contact with a black sandy silt below. It contains shell fragments and brackish and marine diatoms, with some plant debris, suggesting a marine flooding event. The unit above contains fine sand and scarce but predominantly brackish diatoms (< 4%), more than in the sediments below sand unit 4 that show brackish to marine diatoms increasing downward in the slice, indicating a change in environment, probably a minor land-level change, i.e., minor uplift. The time frame of this event is not conclusive, older than 1240–1370 AD (Fig. 2).

Finally, the lowest deformed sand unit 5 with sharp basal contact, shell fragments, and marine diatoms (although diatoms are scarce) suggests probable marine inundation. Deformation of this unit indicates an apparent liquefaction event, most likely produced by an earthquake before 590–666 Cal AD and after 485–359 Cal BC (Fig. 2).

Coastal land-level changes and variable recurrence of large events

In summary, we provide evidence of four tsunamigenic earthquakes, although one of these events has a nonconclusive age (sand unit 4). These four earthquakes produced tsunamis, although only event 3, marked by sand unit 3, produced permanent and remarkable deformation, i.e., coastal subsidence. The other three events apparently produced a slight uplift or minor to nonpermanent deformation. The inland extent of tsunami flooding is a minimum estimate based on the surface distribution of associated deposits. However, given the high velocity and destructive pathways of a tsunami, the source of sediment and preservation of deposits, the 800 m inundation limit is a minimum estimate[23,24,25,26]. The time frame of these events shows that recurrence is highly variable for the past ca. 2000 years (Fig. 2). However, this record has unknown incompleteness and is a maximum estimate of average tsunamigenic earthquakes. Nevertheless, the "1300 AD" event (unit 3) is likely a remarkable event that produced considerable coastal deformation (≥ 1 m subsidence) and may reflect a rupture closer to the trench. Most instrumentally recorded events on the MSZ rupturing near the coast produced coastal uplift for earthquakes in 1962, 1985, and 2020[16,27,28]. However, other large near-trench earthquake events (within 20 km) causing seismic slip in the shallow portion of the MSZ, such as Colima 1995 and Jalisco 1932, produced coseismic coastal subsidence[29,31,32]. Earthquake

ruptures near the trench cause vertical coseismic displacement and uplift, generating tsunamis[33]. Near-trench events in the GS are relatively common, such as the 2002 Mw6.7 near-trench tsunami earthquake, which produced a limited tsunami response (< 10 cm)[34]. Tsunami modeling of a hypothesized near-trench Mw8.4 earthquake produces tsunami amplitudes over 9 m at the coast and inundation over 1 km inland in the study area. This model fits long-term evidence of a Mw>8 earthquake and a tsunami that flooded > 1 km inland (Fig. 6).

Does slow slip inhibit large earthquakes?

Geophysical studies in the GS are based on a limited 113-year time series and measurements of SSEs in the last ~20 years[35,36,37] of instrumental seismic observations. SSEs are hypothesized to reflect trapped fluids, although there is limited evidence of fluids associated with the Guerrero segment and other fault zones. Furthermore, the concept that the rheology of this segment favors slow slip over fast slip[2,3] remains unconstrained. Megathrust earthquakes have ruptured on the same or neighboring sectors of subduction zones where slow slip occurred[4,5,6,38,39]. For instance, two slow slip events in the Japan subduction zone preceded the 2011 Tohoku earthquake, indicating the coexistence of slow slip and earthquakes in the same portion of the subduction zone, such as the Mw9.1 Tohoku earthquake[4]. Other examples of SSE´s preceding large earthquakes were observed in Chile and Mexico in 2012 and 2014. In Chile, an SSE that lasted 2 weeks anticipated the Mw8.2 Iquique earthquake[40]. In Mexico, the SSE initiated four months prior to the 2012 Mw = 7.4 with the Ometepec earthquake moving toward the earthquake source region[41]. Additionally, a Mw7.3 earthquake was preceded by an SSE in the neighboring region of the earthquake source in Guerrero[42]. However, the phenomenon of SSEs and the occurrence of

large earthquakes are still not well understood. Furthermore, geodetic observations in GS have a relatively short period to accurately determine the seismic coupling state and include limited observations of > 8 Mw earthquakes, providing uncertainty in these estimates[43]. Thus, the interplate locking state should be known to infer the occurrence of the potential of a large earthquake[6]. Submarine topographic features offshore Guerrero, such as seamounts and ridges[8,] might also promote an increase in interplate coupling and consequently tsunamigenic earthquakes[10]. Geologic and historical evidence of large earthquakes (Mw> 8), such as those presented here for the GS, provides records that span hundreds to thousands of years, providing minimum estimates on and evaluating large (> 8 Mw) earthquakes and tsunamigenic event potential[44,45,46,47]. Through combined long-term and instrumental observations and a deeper understanding of the relationship between SSEs and rapid slip (earthquake), earthquake and tsunami future occurrences might be better forewarned.

Long-term record of earthquakes vs. short instrumental geophysical observations

Our results show geologic and historical evidence of past large earthquakes coupled with tsunamis in the last 2000 years. A potential large tsunamigenic earthquake (M > 8) in ~1300 AD, i.e., is substantially larger than that recorded instrumentally and observed during the past ca. 110 years. The ages for the four tsunami-indicative sand units are younger than the mid-Holocene sea-level highstand, and sea-level records for the past 2 ka show little to mild changes in sea level, < 1 mm/year, until the late mid-19th century when sea level increased[48]. Previous work on this segment of the MSZ also provided evidence for apparent older earthquakes, probably 3

tsunami events during the past 4600 BP years[7,12]. Evidence of another large earthquake that produced land subsidence accompanied by marine inundation, most likely a tsunami, by *c*. 3400 yr BP, was reported on the Guerrero coast[7]. The neighboring Oaxaca segment shows historical and geologic evidence of a Mw8.6 earthquake and tsunami in the 1787 flooding > 500 km alongshore and up to > 6 km inland[49].

Recent geologic evidence provides new insights into extraordinary catastrophic events in the Mexican subduction zone. Recurrence of large events might be in the range of centuries. Our observations also indicate that indeed subduction zones might have variable rupture modes. The GS and other segments on the MSZ and other subduction zones require combined long-term and instrumental observations to forewarn eventual catastrophes. Our findings offer evidence to prepare communities for earthquake and tsunami hazards.

Methods

Field survey

Field exploration and reconnaissance were performed during several seasons and years, looking for the potential environments that would preserve tsunami deposits. We worked on salt marshes, estuaries, swales between beach ridges, and swamps along 55 km of the coast of the Guerrero segment and used a hang huger, geoslicer, and pits at more than 20 sites (Supplementary Fig. S1). We found evidence of tsunami deposits near estuaries, dug, and collected geoslices as far as 800 m landward (Fig. 1).

Stratigraphic and sediment analysis

We constructed stratigraphic cross sections using geoslices and pits (Fig. 2). Focus was given to sites A1 and A2 for further sediment analysis, including grain size, diatoms, geochemistry and different dating techniques. Site A1 was used to study magnetic properties, including magnetic susceptibility and anisotropy of magnetic susceptibility (AMS).

Diatom analysis

Samples for microfossil (diatoms) analyses were collected from site A1. One gram of dry sediment was sampled from each horizon and dispersed in 10% hydrochloric acid to remove carbonates. Later, these samples were neutralized and dispersed in distilled water. Thin sections were made with 400 µl of liquid dispersion for each slide. Counts of valves were undertaken with a Carl Zeiss (series 470801-9097) microscope, and species composition is reported as total abundance recognized in the slides. Diatom fragments were counted on the same area in all samples under oil immersion with a magnification of 100x; however, diatom valves in some samples (sand layers and clay bed between 21 and 45 cm in A1) were investigated in various thin sections from the same horizons due to scarce diatoms in these horizons. A coarse fraction, larger than the diatom size, was extracted from sand beds before preparation of thin sections to increase the number of possible findings. Each specimen counted no less than half a valve. We identified and counted 1420 diatom valves from site A1. The environmental preferences of the diatoms were determined

based on the literature (Supplemental Information). Microfossil diagrams were created using Tilia software[50].

Anisotropy of magnetic susceptibility analysis

Samples for magnetic susceptibility measurements were collected along a continuous vertical profile from A1 every 2 cm into plastic boxes with a volume of 7 cm^3. Some fabrics were verified in the field by taking natural samples from a pit wall at site A1 because of fabric deformation during coring. Only natural and original fabrics from 4 different units were preserved at site A1. All AMS measurements were conducted using the MFK1-FA Kappabridge device (applied field of 200 A/m) and using a 3D rotator[51]. Principal susceptibility directions $\mathbf{K_1}$, $\mathbf{K_2}$, and $\mathbf{K_3}$ correspond to maximum, intermediate, and minimum susceptibility directions, respectively. AMS parameters *T* (shape parameter) and *P* (degree of anisotropy) have been defined by Jelinek[52,53].

210 Pb dating and elemental composition, OSL and C14 analysis

We used the same technique described by Ramirez-Herrera et al.[49] for elemental composition analysis and 210Pb chronology. The top sediment sequence, from 1 to 25 cm, of which only the first 16 cm was measured for this purpose, the rest were beyond the range of datable material using the CFCS model. Thus, the dated sequence was very young, 40 years old (Supplementary

Table S1). Fourteen samples for radiocarbon dating were measured and dated at the Beta Analytic Laboratory (Supplementary Table S2).

Optical stimulated luminescence (OSL) analysis was performed at the Geoluminiscence Research Dating Lab facility at Baylor University. Collection of samples was performed as described by the facility (https://www.baylor.edu/geosciences/index.php?id=955930). Three samples were measured for OSL dates (Supplementary Table S3).

Tsunami modeling

Tsunami modeling was computed using the Geowave code[54]. A hypothetical Mw = 8.4 earthquake was positioned in the middle of the Guerrero segment and defined with a rupture area of 180 × 90 km^2 at a depth of 20 km (detailed input in Supplementary Table S4). The first step in the code, TOPICS, solves the initial coseismic deformation and transfers it to the free water surface. This step is driven by the elastic half-space formulation of Okada[55]. The propagation and inundation modeling were solved by the subroutine FUNWAVE, a fully nonlinear Boussinesq model. The simulation time was established at 120 minutes at one-minute intervals. The input for the propagation and inundation tsunami model was the topo-bathymetric model version GEBCO_2022, provided for GEBCO Compilation Group, GEBCO_2022 Grid a Global grid[56] of elevation values in meters on a 15 arc-second interval grid, equivalent to ca. 453 m, and land topographic data from a 5 m LIDAR Digital Terrain Model.

References

1. Suarez, G., Montfret, T., Wittlinger, G. & David, C. Geometry of subduction and depth of the seismogenic zone in the Guerrero Gap, Mexico. *Nature* 345, 336–38 (1990).

2. Husker, A., Werner, M. J., Bayona, J. A., Santoyo, M. & Corona-Fernandez, R. D.. A Test of the Earthquake Gap Hypothesis in Mexico: The Case of the Guerrero Gap. *Bull. Seismol. Soc. Am.* XX, 1–12 (2022). Doi: 10.1785/ 0120220094

3. Husker, A., Ferrari, L., Arango-Galván, C., Corbo-Camargo, F. & Arzate-Flores, J. . A geologic recipe for transient slip within the seismogenic zone: Insight from the Guerrero seismic gap, Mexico. *Geology* 46 (1), 35–38. (2018). https://doi.org/10.1130/G39202.1

4. Ito, Y., Hino, R., Kido, M., Fujimoto, H., Osada, Y., Inazu, D., Ohta, Y., Iinuma, T., Ohzono, M., Miura, S. & others. Episodic slow slip events in the Japan subduction zone before the 2011 Tohoku-Oki earthquake. Tectonophysics 600, 14–26 (2013). http://dx.doi.org/10.1016/j.tecto.2012.08.022

5. Obara, K. & Kato, A. Connecting slow earthquakes to huge earthquakes. *Science* **353**, 253–257 (2016).

6. Uchida, N. & Bürgmann, R. A decade of lessons learned from the 2011 Tohoku-Oki earthquake. Reviews of Geophysics 59, e2020RG000713 (2021).https://doi.org/10.1029/2020RG000713

7. Ramírez-Herrera, M.T., Cundy, A., Kostoglodov, V., Carranza-Edwards, A., Morales, E. & Metcalfe, S. Sedimentary record of late Holocene relative sea-level change and tectonic deformation from the Guerrero Seismic Gap, Mexican Pacific Coast. *The Holocene.* 17(8):1211-1220 (2007)**.** https://doi.org/10.1177/0959683607085127

8. Černý, J., Ramírez-Herrera, M. T., Garcia, E., Ito, Y. Seafloor morphology along the active margin in Guerrero, Mexico: Probable earthquake implications. *Journal of South American Earth Sciences* 102 (2020). https://doi.org/10.1016/j.jsames.2020.102671.

9. Bell, R., Holden, C., Power, W., Wang, X, & Downes, G. Hikurangi margin tsunami earthquake generated by slow seismic rupture over a subducted seamount. *Earth Planet. Sci. Lett.* 397, 1–9 (2014). https://doi.org/10.1016/j.epsl.2014.04.005

10. Prada, M., Bartolomé, R., Gras, C., Bandy, W. & Dañobeitia, J. J. Trench-parallel ridge subduction controls upper-plate structure and shallow megathrust seismogenesis along the Jalisco-Colima margin, Mexico. *Commun Earth Environ* 4, 53 (2023). https://doi.org/10.1038/s43247-023-00705-9

11. Servicio Mareográfico Nacional: https://chalchiuhtlicue.geofisica.unam.mx/

12. Ramírez-Herrera, M.T., Cundy, A. & Kostoglodov, V. Probables sismos y tsunamis prehistóricos durante los últimos 5000 años en la costa de la brecha sísmica de Guerrero, México. *XV CNIS Sociedad Mexicana de Ingeniería Sísmica.* I-07:1-17 (2005).

13. Dolman, A. M., Groeneveld, J., Mollenhauer, G., Ho, S. L., & Laepple, T. Estimating bioturbation from replicated small-sample radiocarbon ages. *Paleoceanography and Paleoclimatology* 36 (7), e2020PA004142 (2021).

14. Černý, J. Ramírez-Herrera, M.T. & Caballero, M. Procedures for diatom analyses and hydrodynamic separation of extreme wave paleo-deposits from tropical sediment environments. *Marine Geology* 455,106970, (2023). Doi.org/10.1016/j.margeo.2022.106970

15. Tarling, D. H. & Hrouda, F. The magnetic anisotropy of rocks. *Champan and Hall,* London, United Kingdom, (1993)

16. Ortiz, M., Singh, S. K., Kostoglodov, V., & Pacheco J. Source areas of the Acapulco-San Marcos, Mexico earthquakes of 1962 (*M* 7.1; 7.0) and 1957 (*M* 7.7), as constrained by tsunami and uplift records. *Geofísica Internacional* 39 (4), 337-348 (2000).

17. Wassmer, P., Schneider, J.L., Fonfrège, A.V., Lavigne, F., Paris, R. & Gomez, C. Use of anisotropy of magnetic susceptibility (AMS) in the study of tsunami deposits: Application to the 2004 deposits on the eastern coast of Banda Aceh, North Sumatra, Indonesia. *Marine Geology* 275, 255–272 (2010). doi:10.1016/j.margeo.2010.06.007

18. Cuven, S., Paris, R., Falvard, S., Miot-Noirault, E., Benbakkar, M., Schneider, J. L. & Billy, I. High-resolution analysis of a tsunami deposit: Case-study from the 1755 Lisbon tsunami in southwestern Spain. *Marine Geology* 337, 98–111 (2013). Doi:10.1016/j.margeo.2013.02.002

19. Schneider, J. L., Chagué-Goff, C., Bouchez, J. L., Goff, J., Sugawara, D., Goto, K., Jaffe, B. & Richmond, B. Using magnetic fabric to reconstruct the dynamics of tsunami deposition on the Sendai Plain, Japan – The 2011 Tohoku-oki tsunami. *Marine Geology* 358, 89–106 (2014). Doi:10.1016/j.margeo.2014.06.010

20. Černý, J., Ramírez-Herrera, M. T., Bógalo, M. F., Goguitchaichvili, A., Castillo-Aja, R., Morales, J., Sanchez-Cabeza, J.A. & Ruiz-Fernández, A.Magnetic record of extreme marine inundation events at Las Salinas site, Jalisco, Mexican Pacific coast. *International Geology Review* 58, 3 (2016). http://dx.doi.org/10.1080/00206814.2015.1075230

21. Suárez, G. Catálogo de Sismos Históricos de México. (2021). http://www.sismoshistoricos.org/

22. Ramírez-Herrera, M.-T., Corona, N. & Suárez, G. A Review of Great Magnitude Earthquakes and Associated Tsunamis along the Guerrero, Mexico Pacific Coast. In Extreme

Events (eds M. Chavez, M. Ghil and J. Urrutia-Fucugauchi). (2015). https://doi-org.pbidi.unam.mx:2443/10.1002/9781119157052.ch13

23. Abe, T., Goto, K. & Sugawara, D. Relationship between the maximum extent of tsunami sand and the inundation limit of the 2011 Tohoku-oki tsunami on the Sendai Plain, Japan. *Sediment Geol* 282:142–150 (2012). https://doi.org/10.1016/j.sedgeo.2012.05.004

24. Abe, T., Goto, K. & Sugawara, D. Spatial distribution and sources of tsunami deposits in a narrow valley setting-insight from 2011 Tohoku-oki tsunami deposits in northeastern Japan. Progress in Earth and Planetary Science 7, 1–21 (2020). https://doi.org/10.1186/s40645-019-0318-6

25. Moreira, S., Costa, P. J., Andrade, C., Lira, C. P., Freitas, M. C., Oliveira, M. A. & Reichart, G.-J. High resolution geochemical and grain-size analysis of the AD 1755 tsunami deposit: Insights into the inland extent and inundation phases. Marine Geology 390, 94–105 (2017). https://doi.org/10.1016/j.margeo.2017.04.007

26. Shinozaki, T., Sawai, Y., Ikehara, M., Matsumoto, D., Shimada, Y., Tanigawa, K. & Tamura, T. Identifying tsunami traces beyond sandy tsunami deposits using terrigenous biomarkers: a case study of the 2011 Tohoku-oki tsunami in a coastal pine forest, northern Japan. Progress in Earth and Planetary Science 9, 1–10 (2022). https://doi.org/10.1186/s40645-022-00491-6

27. Bodin, P. & Klinger, T. Coastal uplift and mortality of intertidal organisms caused by the September 1985 Mexico earthquakes. Science 233, 1071–1073 (1986).

28. Ramírez-Herrera, M.T., Romero, D., Corona, N, Nava, H. The 23 June 2020 Mw 7.4 La Crucecita, Oaxaca, Mexico Earthquake and Tsunami: A Rapid Response Field Survey during COVID-19 Crisis. Seismological Research Letters. 92. (2020). 10.1785/0220200263.

29. Cumming, J. L. Los terremotos de Junio de 1932 en los estados de Colima y Jalisco. Universidad de México 6, 68–104 (1933).

30. Hutton, W., DeMets, C., Sanchez, O., Suarez, G. & Stock, J. Slip kinematics and dynamics during and after the 1995 October 9 Mw= 8.0 Colima–Jalisco earthquake, Mexico, from GPS geodetic constraints. Geophysical Journal International 146, 637–658 (2001). https://doi.org/10.1046/j.1365-246X.2001.00472.x

31. Hjörleifsdóttir, V., Sánchez-Reyes, H. S., Ruiz-Angulo, A., Ramírez-Herrera, M. T., Castillo-Aja, R., Singh, S. K. & Ji, C. Was the 9 October 1995 Mw 8 Jalisco, Mexico, Earthquake a Near-Trench Event? Journal of Geophysical Research: Solid Earth 123, 8907–8925 (2018). Doi: 10.1029/2017JB014899

32. Pacheco, J., S. K. Singh, J. Domínguez, A. Hurtado, L. Quintanar, Z. Jiménez, J. Yamamoto, C. Gutiérrez, M. Santoyo, W. Bandy, M. Guzmán, V. Kostoglodov, G. Reyes And C. Ramírez. The October 9, 1995 Colima-Jalisco, Mexico earthquake (Mw 8): An aftershock study and a comparison of this earthquake with those of 1932. Geophys. Res. Lett., 24, 2223-2226 (1997).

33. Kanamori, H., and M. Kikuchi. The 1992 Nicaragua earthquake: A slow tsunami earthquake associated with subducted sediments, *Nature*, **361**, 714–716 (1993), doi:10.1038/361714a0.

34. Flores, K., Hjorleifsdottir, V., Iglesias, A. & Singh, S. Did the Long Duration, April 18, 2002 (Mw 6.7), Mexico Earthquake Break the Guerrero Gap? in AGU Fall Meeting Abstracts 2016, S53A–2803 (2016). 2016AGUFM.S53A2803F

35. Kostoglodov, V., Singh, S., Santiago, J., Franco, S., Larson, K., Lowry, A. & Bilham, R. . A large silent earthquake in the Guerrero seismic gap, Mexico. *Geophys. Res. Lett.*, **30**(15), 1807 (2003). Doi:10.1029/2003GL017219.

36. Larson, K., Kostoglodov, V., Miyazaki, S. & Santiago, J. A. The 2006 aseismic slow slip event in Guerrero, Mexico: New results from GPS. *Geophys. Res. Lett.*, **34**, L13309 (2007). Doi:10.1029/2007GL029912

37. Radiguet, M., Cotton, F., Vergnolle, M., Campillo, M., Walpersdorf, A., Cotte, N. & Kostoglodov, V. Slow slip events and strain accumulation in the Guerrero gap, Mexico. *J. Geophys. Res.* 117, no. B4 (2012). Doi: 10.1029/2011JB008801.

38. Kato, A., Obara, K., Igarashi, T., Tsuruoka, H., Nakagawa, S. & Hirata, N. Propagation of slow slip leading up to the 2011 M w 9.0 Tohoku-Oki earthquake. Science 335, 705–708 (2012).

39. Yokota, Y. & Koketsu, K. A very long-term transient event preceding the 2011 Tohoku earthquake. Nature communications 6, 5934 (2015).

40. Ruiz, S., Metois, M., Fuenzalida, A., Ruiz, J., Leyton, F., Grandin, R., Vigny, C., Madariaga, R. & Campos, J. Intense foreshocks and a slow slip event preceded the 2014 Iquique M w 8.1 earthquake. Science 345, 1165–1169 (2014).

41. Graham, S. E., DeMets, C., Cabral-Cano, E., Kostoglodov, V., Walpersdorf, A., Cotte, N., Brudzinski, M., McCaffrey, R. & Salazar-Tlaczani, L. GPS constraints on the 2011–2012 Oaxaca slow slip event that preceded the 2012 March 20 Ometepec earthquake, southern Mexico. Geophysical Journal International 197, 1593–1607 (2014).https://doi.org/10.1093/gji/ggu019

42. Radiguet, M., Perfettini, H., Cotte, N., Gualandi, A., Valette, B., Kostoglodov, V., Lhomme, T., Walpersdorf, A., Cabral Cano, E. & Campillo, M. Triggering of the 2014 M w 7.3 Papanoa earthquake by a slow slip event in Guerrero, Mexico. Nature Geoscience 9, 829–833 (2016). https://doi-org.pbidi.unam.mx:2443/10.1038/ngeo2817

43. Rousset, B., Lasserre, C., Cubas, N., Graham, S., Radiguet, M., DeMets, C., Socquet, A., Campillo, M., Kostoglodov, V., Cabral-Cano, E. & others. Lateral variations of interplate coupling along the Mexican subduction interface: Relationships with long-term morphology and fault zone mechanical properties. Pure and Applied Geophysics 173, 3467–3486 (2016).

44. Minoura, K. & Nakaya, S. Traces of tsunami preserved in inter-tidal lacustrine and marsh deposits: some examples from northeast Japan. The Journal of Geology 99, 265–287 (1991).. https://doi.org/10.1086/629488

45. Atwater, B. F., Nelson, A. R., Clague, J. J., Carver, G. A., Yamaguchi, D. K., Bobrowsky, P. T., Bourgeois, J., Darienzo, M. E., Grant, W. C., Hemphill-Haley, E. & others. Summary of coastal geologic evidence for past great earthquakes at the Cascadia subduction zone. Earthquake spectra 11, 1–18 (1995).

46. Sawai, Y., Namegaya, Y., Okamura, Y., Satake, K. & Shishikura, M. Challenges of anticipating the 2011 Tohoku earthquake and tsunami using coastal geology. Geophysical Research Letters 39, (2012). https://doi.org/10.1029/2012gl053692

47. Sugawara, D., Imamura, F., Goto, K., Matsumoto, H. & Minoura, K. The 2011 Tohoku-oki earthquake tsunami: similarities and differences to the 869 Jogan tsunami on the Sendai plain. Pure and Applied Geophysics 170, 831–843 (2013). https://doi.org/10.1007/s00024-012-0460-1

48. Kemp, Andrew C., et al. "Climate related sea-level variations over the past two millennia." *Proceedings of the National Academy of Sciences* 108.27 11017-11022 (2011). 10.1073/pnas.1015619108

49. Ramírez-Herrera, M.-T., Corona, N., Cerny, J., Castillo-Aja, R., Melgar, D., Lagos, M., Goguitchaichvili, A., Machain, M. L., Vazquez-Caamal, M. L., Ortuño, M. & others. Sand

deposits reveal great earthquakes and tsunamis at Mexican Pacific Coast. Scientific Reports 10, 11452 (2020). https://doi.org/10.1038/s41598-020-68237-2

50. Grimm E.C., 2016. Tilia software; ver. 2.0.60. Available from: https://www.tiliait.com/

51. Studỳnka, J., Chadima, M. & Suza, P. Fully automated measurement of anisotropy of magnetic susceptibility using 3D rotator. Tectonophysics 629, 6–13 (2014). doi:10.1016/j.tecto.2014.02.015

52. Jelinek, V. Characterization of the magnetic fabric of rocks. Tectonophysics 79, T63–T67 (1981). doi:10.1016/0040-1951(81)90110-4

53. Nagata, T. Rock magnetism (second edition). — Tokyo, Maruzen Company Ltd., 350 Pages (1961).

54. Watts, P., Grilli, S. T., Kirby, J. T., Fryer, G. J., & Tappin, D. R. Landslide tsunami case studies using a Boussinesq model and a fully nonlinear tsunami generation model. *Natural hazards and earth system sciences*, *3*(5), 391-402 (2003).

55. Okada, Y. Surface deformation due to shear and tensile faults in a half-space. *Bulletin of the seismological society of America*, *75*(4), 1135-1154 (1985).

56. GEBCO_2022, GEBCO Compilation Group, GEBCO_2022 Grid (2022), doi:10.5285/e0f0bb80-ab44-2739-e053-6c86abc0289c.

Acknowledgements

We thank Tina Dura for significant feedback and valuable discussions. Diatom analyses were performed at Laboratorio de Micropaleontlogía y Paleoceanografía del Instituto de Ciencias del Mar y Limnología -UNAM. We are indebted to A. Rodriguez R. technician at M&P-ICMyL for assisting with microfossil analysis. AMS analysis were performed at Laboratorio

Interinstitucional de Magnetismo Natural – UNAM, with assistance by Miguel Cervantes. D. Romero-Hernández, V. Vargas-Espinoza, and O. Coca provided helpful assistance during field work. This research project was funded by CONACYT-284365 and PAPIIT- IN101721 awarded to M.T.R-H.

Contributions

M.T.R-H. conceived and carried out the research, data acquisition, lab analyses, and prepared the manuscript. J.C performed diatom and AMS analysis and helped in field work. N.C. carried out tsunami modelling and created all final figures. K.G. drafted a figure and aided in data interpretation. D.S. aided in initial subsampling, helped with data interpretation. All authors mentioned above participated in field work. S.F. carried out OSL analysis. M.M-C. assisted with microfossil identification. A.G. assisted in AMS analysis. All authors discussed the results and revised the manuscript.

Data availability statement

No datasets were generated or analysed during the current study.

Conflicts of Interest Statement

We have no conflicts of interest to disclose. We state that no humans were involved during field survey, or any questionnaire has been conducted for information regarding the study.

Figures

Figure 1. Tectonic and seismic setting of the Mexican Subduction zone. a – Large earthquakes (M>6.5) of the last century and rupture areas along the Mexican subduction zone. b - Guerrero segment, image shows topographic roughness on the subducting Cocos plate, c - Location of studied sites A1 and A2 along the Guerrero coast.

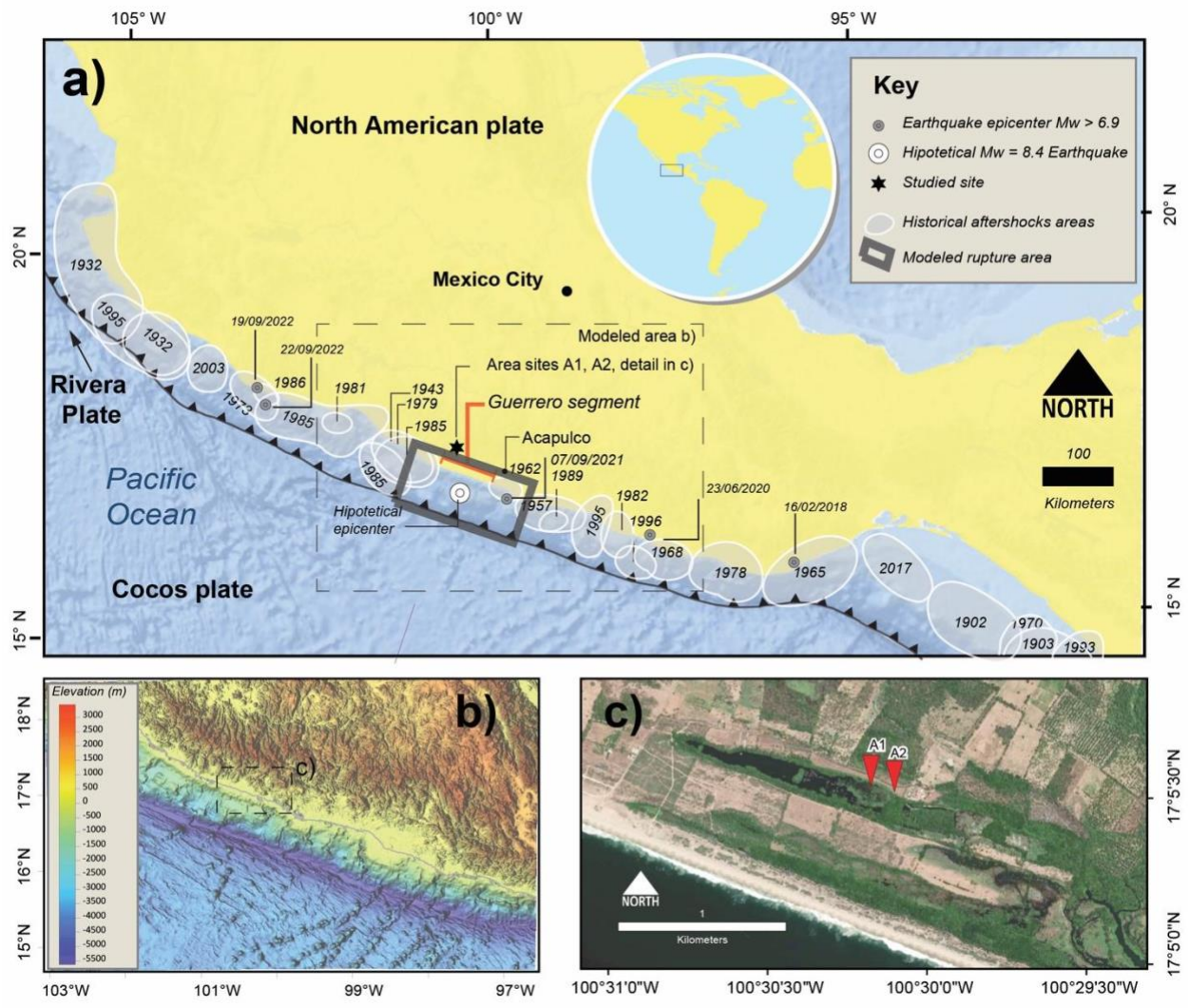

Figure 2. Sites A1 and A2 showing lab-based logged stratigraphy. Correlated sand units marked with dashed lines at the two sites. ^{14}C (gray font), ^{210}Pb (black font), and OSL (green font) dates are shown next to the logs at A1 and A2. Sand units 2, 3, 4 and 5 represent tsunami events of the last 2000 years.

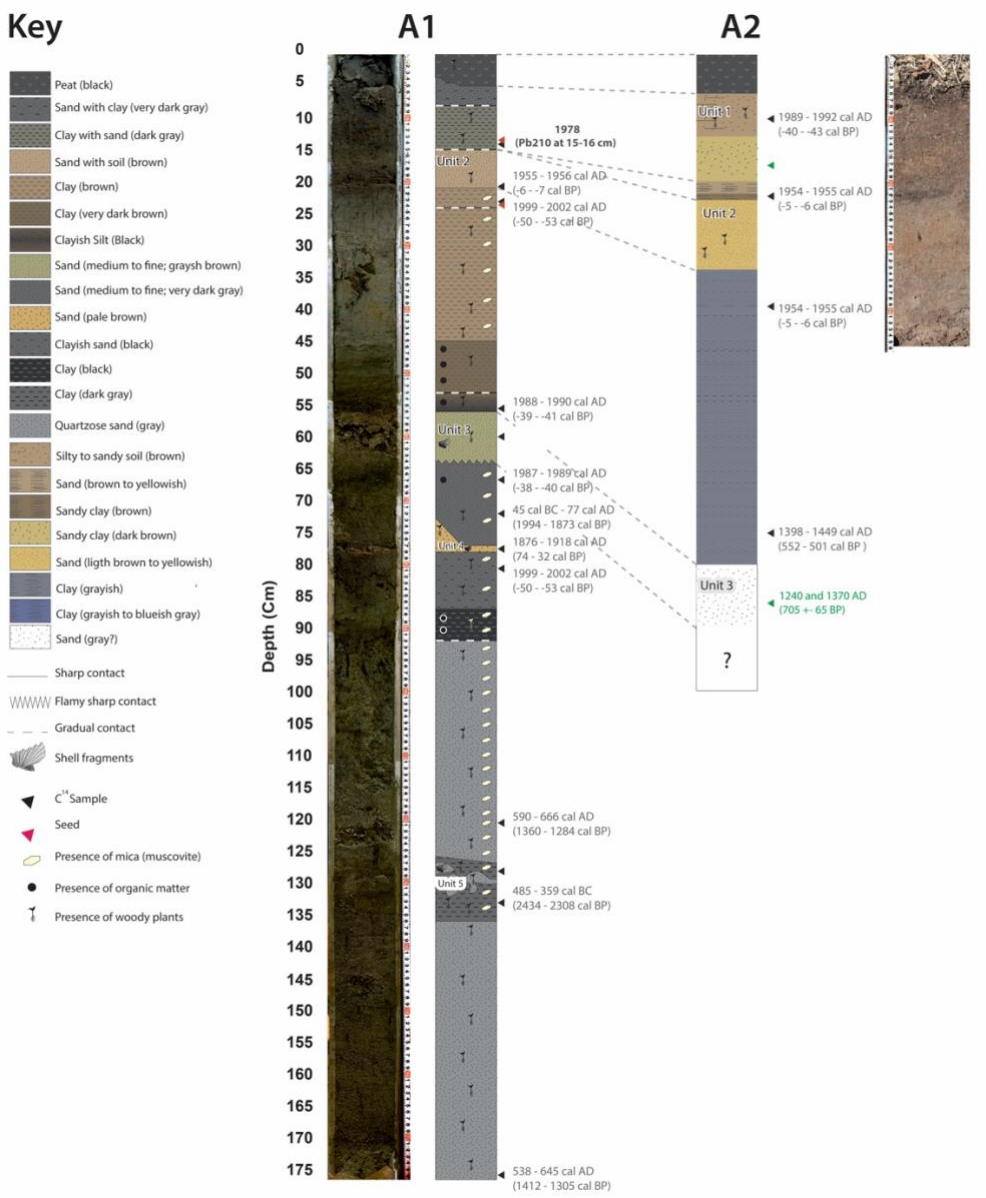

Figure 3. Synoptic results of microfossil analyses for site A1. Colors indicate depositional environments. The relative abundance of diatoms is given as a percent of the total count. A1 stratigraphic column to the left shows sand units 2, 3, 4 and 5. Blue belts show inferred tsunami events.

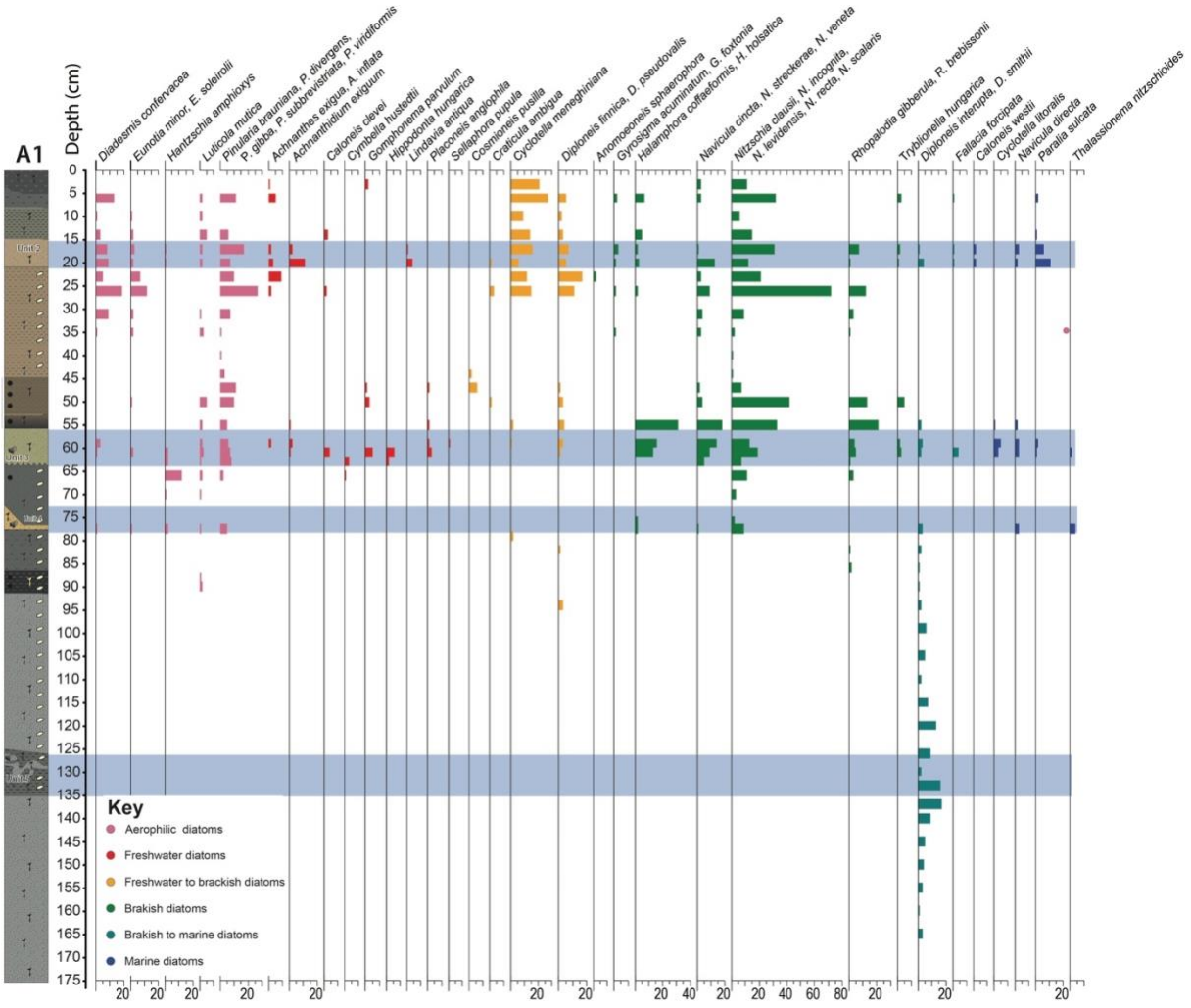

Figure 4. Site A1 anisotropy of magnetic susceptibility (AMS), magnetic fabrics, and magnetic susceptibility of plotted together with the stratigraphic column. AMS Fabric I and III show flow direction and high energy flooding events – tsunamis.

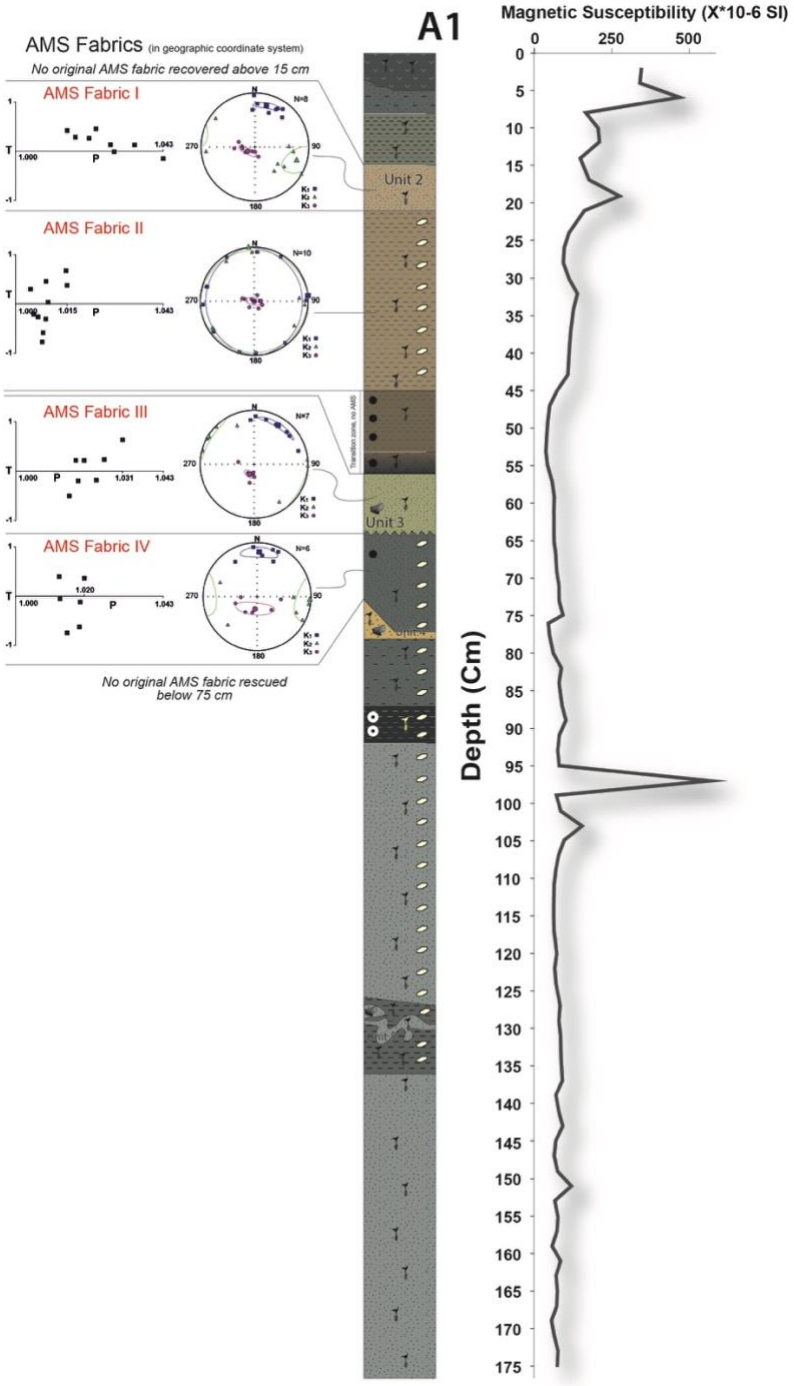

Figure 5. Coastal modern environments determined by diatom analysis on a transect from the coast and inland at study site A1. a - Topographic profile and associated landforms; b - Summary of diatom content by predominant species showing local ecology (represented in colors) and associated coastal landforms.

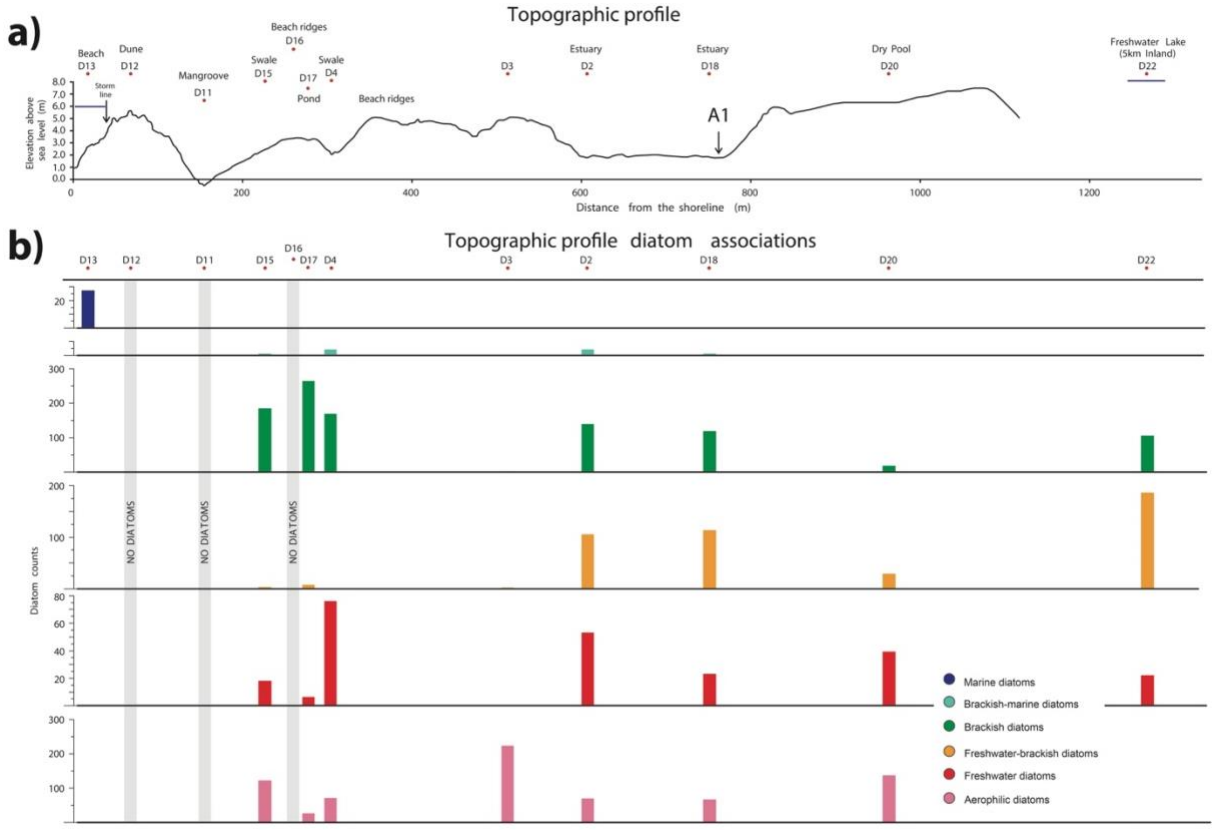

Figure 6. Tsunami model of a hypothesized Mw 8.4 earthquake near the trench producing a tsunami with amplitudes over 9 m at the coast and inundation over 1 km inland at the studied area A1- a; b - Close-up to tsunami inundation depths at the studied area where sites A1 and A2 preserve tsunami deposits from the 1300 AD tsunamigenic earthquake. c - Tsunami amplitudes along the Guerrero segment of the Pacific coast of Mexico.

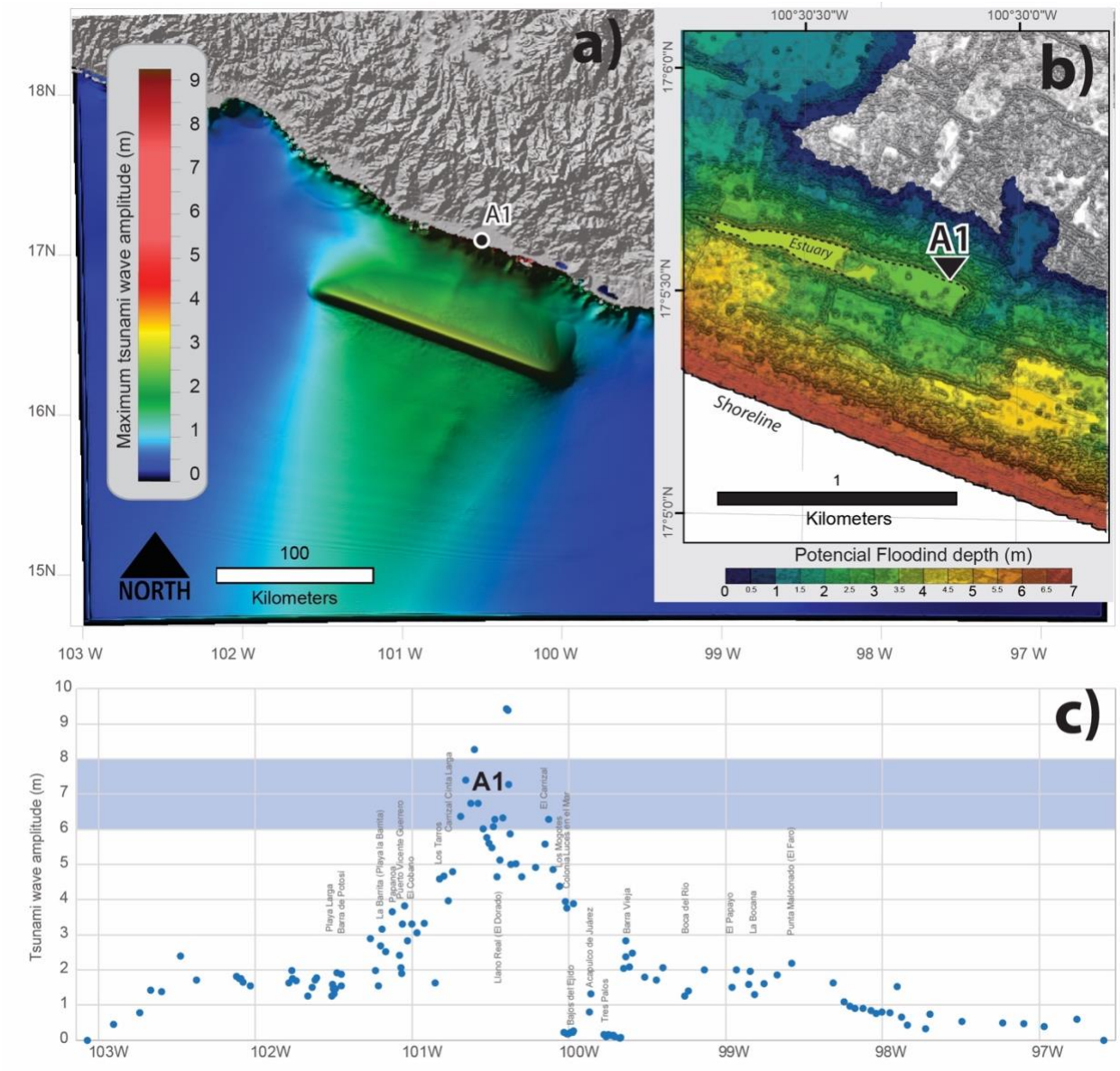

Supplementary information

This file contains Supplementary Figures S1-S4 with Legends, Supplementary Tables S1-S4 and Supplementary Notes